An aero-elastic flutter based electromagnetic energy harvester with wind speed augmenting funnel

Jin-Kyoo Park[1], Kyoung-Min Kim[2], Soon-Dock Kwon[3] and Kincho H. Law[4]

[1), 4)] *Dept. of Civil and Environmental Engineering, Stanford University, USA*
[2), 3)] *Dept. of Civil Engineering, Chonbuk National University, Korea.*
[1)] *jkpark11@stanford.edu*

ABSTRACT

This paper investigates the efficiency of wind speed augmenting funnel incorporated with an aero-elastic-flutter based, energy harvester. Flutter phenomenon has been used to convert wind flow energy into mechanical vibration, which is then transformed into electrical power. However, aero-elastic flutter initiates only when the wind speed is over a certain flutter onset speed and the wind flow direction is nearly perpendicular to the device, which limits continuous power generation. A wind-flow-contracting funnel device is designed to direct the wind flow to the flutter device and magnify the wind speed. The preliminary CFD analysis and wind tunnel test show that the funnel can magnify wind speed by approximately 20 % within an incident angle of 30 degrees, which leads to an increase in the voltage output of the device.

1. INTRODUCTION

Energy harvesting has been an active research area as demands for renewable energy sources increase. Energy harvesting systems refer to devices that capture and transform energy from the environment into electricity. Unlike conventional, large-scale renewable energy generating systems such as wind turbines, thermal generators, and solar panels, energy harvesting devices mostly target on powering small electronic devices. For example, many researchers are investigating how to supply power to wireless sensor modules using energy harvesters (Roundy 2004). If such sensors can be operated solely on power generated from an energy harvester, the needs for regularly changing batteries can be eliminated, and the maintenance cost of wireless sensor network can thus be reduced.

Vibration-based energy harvesters, which are the focus of this paper, can be categorized into three types, namely electromagnetic, piezoelectric, and electrostatic, depending on the medium of the transducer (Beeby 2006). The transducers require input vibration with high frequency to generate electricity. Civil structures exhibit usually low frequency structural vibrations, which make it difficult for an energy harvester to extract energy. To overcome this limitation, we use wind-induced flutter vibration as an alternate input source and convert the mechanical energy into electricity using an electromagnetic transducer. We also propose wind flow contracting funnel to increase the efficiency of the flutter-based energy harvester.

[1)] Graduate Student [2)] Graduate Student [3)] Professor [4)] Professor

2. THEORETICAL BACKGOURND

2.1. Wind as a source for energy harvesting

Wind energy has long been used to generate power mostly using wind turbines by exploiting the blades' lift and drag forces to rotate an electromagnetic generator. This conventional approach for generating power is, however, difficult to apply to small scale energy harvesters, because small size generators are difficult to make and have low efficiency. Wind induced vibrations have been used as an alternate input source for small scale energy harvesters. Wind induced vibrations have been used to mechanically strain piezoelectric transducers to generate power (Allen 2001, Sun 2011) and to generate inductance power in electromagnetic transducers (Jung 2011). Aero-elastic instability phenomenon, which is referred to as flutter, has also been suggested as an input source for energy harvesters because of its potential capacity for generating electrical power. Flutter induced vibration of T-shape cantilever beam and plate have been used to mechanically strain piezoelectric patches to generate power (Kwon 2010, Bryant 2011). A leaf-like structure has also been proposed to convert cross-flow flutter into electricity using Poly Vinylidene Fluoride (Li 2011).

Wind possesses many advantages as a renewable energy source. Particularly, generating energy by wind does not depend on a dominant-frequency; as a result, the natural frequency of the vibrating structural part does not need to match a certain frequency, which results in great flexibility in the configuration of energy harvesters. Wind, however, poses many challenges that must be addressed in order for wind to be used as a reliable input source for energy harvesters. These challenges include intermittency which hinders continuous energy production and inconsistent quality of wind flows that reduces the efficiency of energy harvesters. The intermittency problem can be overcome if the generated power is sufficiently large for storage in batteries. Regarding to the second problem, the quality of wind flows, we evaluate a wind flow contracting funnel applied to the flutter based energy harvester in this paper.

2.2. Principle of electromagnetic transducer

We first introduce the basic principles of an electromagnetic transducer, which is used to convert flutter induced vibration into electricity. The voltage induced in the electromagnetic transducer is expressed by the Faraday's law as follows:

$$V = -N \frac{d\phi}{dz} \frac{dz}{dt}$$

(1)

where z is the relative displacement between a magnet and the coil and N is the number of coil turns, and ϕ is the magnetic flux. That is, the induced voltage is proportional to the product of a magnetic gradient, which is determined by the geometries of the coil and the magnet as well as their relative configurations, and the relative velocity between the magnet and the coil.

Most electromagnetic based energy harvesters use an inertial frame configuration, in which the relative movement between the magnets and the coils are induced by the vibration of the inertial frame. The vibration system can be described as a second-order differential equation as follows:

$$m\ddot{z}(t) + c\dot{z}(t) + kz(t) = -m\ddot{y}(t) \tag{2}$$

where m, c and k are, respectively, the mass, damping and stiffness of the vibration frame, and $y(t)$ represents the inertial frame displacement. The total extracted power from the vibrating system is equivalent to the dissipated energy by the total damping c_T as follows:

$$P_{avg}(\omega) = \frac{m\zeta_T Y^2 \left(\dfrac{\omega}{\omega_n}\right)^3 \omega^3}{\left[1 - \left(\dfrac{\omega}{\omega_n}\right)^2\right]^2 + \left[2\zeta_T \left(\dfrac{\omega}{\omega_T}\right)\right]^2} \tag{3}$$

where ζ_T is the total damping ratio $(\zeta_T = c_T/2m\omega_n)$, which includes both the mechanical and the transduction damping mechanisms $(\zeta_T = \zeta_M + \zeta_E)$; furthermore, Y, ω and ω_n are, respectively, the maximum displacement, the excitation frequency of the inertial frame and the natural frequency of the vibrational part (Beeby 2007).

The maximum energy dissipation occurs when the exciting frequency coincides with the natural frequency of the system; in this case, the maximum average power becomes

$$P_{avg,\max} = \frac{m\zeta_T Y^2 \omega_n^3}{4\zeta_T^2} \tag{4}$$

The amount of power generated by electromagnetic transduction is equivalent to the dissipated energy by the electromagnetic induction as

$$P_{electric} = \frac{m\zeta_E Y^2 \omega_n^3}{4(\zeta_M + \zeta_E)^2} \tag{5}$$

where $\zeta_E = c_E/2m\omega_n$ and the electric damping coefficient c_E can be expressed as

$$c_E = \frac{(NlB)^2}{R_L + R_C + j\omega L_C} \tag{6}$$

where $N \cdot l$ and B are, respectively, the effective length of the coil and the average flux density; furthermore, R_L, R_C and L_C are, respectively, the load resistance, coil resistance and coil inductance (El-hami 2001).

Based on Eq. (5), we can infer that the maximum power is delivered to the electric part when the electrical damping and mechanical damping are the same ($\zeta_M = \zeta_E$). The maximum average power delivered to the load can thus be expressed as

$$P_{Load} = \frac{mY^2\omega_n^3}{16\zeta_E}\left(\frac{R_L}{R_L + R_C}\right)$$

(7)

In Eq. (7), the factor $R_L/(R_L + R_C)$ represents the fraction of energy transferred to the load from the total extracted energy by all the electrical components. The maximum power transferred to the load occurs when $R_L = R_C$, assuming coil inductance is negligible. It should also be noted that R_L and R_C change the total extracted power by changing the electric damping coefficient c_E.

2.3. Flutter based energy generation

Different from the conventional inertial-frame-based energy harvesters, flutter-based energy harvesters utilize vibrations caused by aero-elastic instability. The equation describing the fluttering vibration of bridges is available in many references (Ge 2000, Scanlan 1978, Wright 2007). The vibration of an n-degree of freedom structure caused by flutter can be written as [7] :

$$[M_S]\{\ddot{\delta}\} + [C_S]\{\dot{\delta}\} + [K_S]\{\delta\} = \{F\}$$

(8)

where $\{\delta\}$ is the displacement vector, $[M_S]$, $[C_S]$ and $[K_S]$ are, respectively, the structural mass, damping and stiffness matrices, and $\{F\}$ is the self excitation force term due to the structural motion in response to wind flow. The self excitation force is given as

$$\{F\} = \{F_D\} + \{F_S\} = [A_D]\{\dot{\delta}\} + [A_S]\{\delta\}$$

(9)

where $\{F_D\}$ and $\{F_S\}$ represent the aerodynamic damping and stiffness forces, respectively; $[A_D]$ and $[A_S]$ are, respectively, aerodynamic damping and stiffness matrices. The matrices $[A_d]$ and $[A_s]$ depend on wind speed, structural geometries, and flutter derivatives relating the aerodynamic forces and wind speed. The flutter derivatives are usually obtained by wind tunnel tests or CFD simulations. Combining Eq. (8) and Eq. (9) gives the equation describing flutter vibration with a damped free vibrational motion as follows (Ge 2000):

$$[M_S]\{\ddot{\delta}\} + ([C_S] - [A_d])\{\dot{\delta}\} + ([K_S] - [A_s])\{\delta\} = \{0\}$$

(10)

Substituting a constant amplitude harmonic solution $\{q(t)\} = \{q_0\}e^{i\omega t}$ into Eq. (10) results in an eigenvalue problem, from which the critical flutter wind speed, which is the

boundary wind speed differentiating a stable and an unstable system, and the corresponding flutter oscillating frequency can be obtained (Staerdhal 2007). Specifying the steady state tip displacement D, which is restricted by a structural member geometry and support condition of energy harvester, we can approximate the vibration of the cantilever tip as $z(t) = D\sin\omega t$. The possible power output of a flutter energy harvester is simply equal to the dissipated energy by the electric transducer damping coefficient c_E as follows

$$P_{avg} = \frac{1}{2}c_E \dot{z}_{\max}^2 \tag{11}$$

where $\dot{z}_{\max}$ is the maximum relative speed between a magnet and a coil.

2.4. Power output measurement for a flutter based energy harvester

Flutter phenomenon can be effectively used to convert wind energy into electricity, since the deflection caused by flutter is large and the oscillating frequency of the flutter is adjustable. To understand the power output characteristics of flutter-based energy harvesters, we conducted a simple experiment using a hair dryer in the laboratory (Fig. 1a) and a field experiment on a highway overpass along the I-280 freeway in the city of Menlo Park, CA. USA (Fig. 1b). As shown, we used T-shape cantilever beam to induce aero-elastic buffering force on the top and the bottom of the cantilever beam.
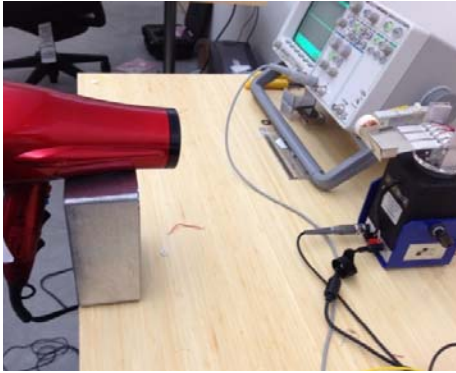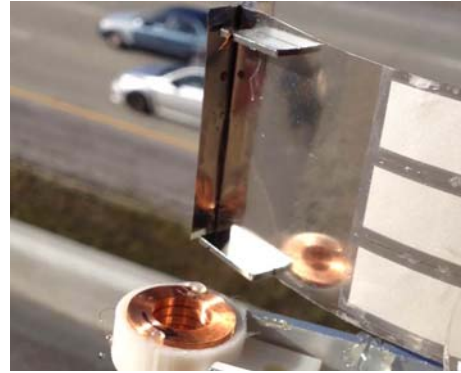
| (a) Laboratory test | (b) Field test |

Fig. 1 Laboratory and field test

We measured the voltage output of the electromagnetic energy transducer by changing load resistance in the lab. Flutter initiates after few seconds of consistent wind blowing into the device. The amplitude of tip displacement increases until it reaches its steady state motion, which almost resembles harmonic forced vibration. The 1-min RMS values for measured voltage and power are summarized in Fig. 2. The hair dryer used in the lab experiment operates with two speeds. The general voltage and power levels are higher when the wind speed is high. Also, the voltage and power level depending on load resistances follow the almost identical trends for inertial-based electromagnetic transducer having the peak power output around $R_L = R_C(600\Omega)$ as

described by Eq. (7). Note that the wind speed is not measured and the purpose of this experiment is to verify the output trends of the flutter energy harvester. If we restrict our interest to the power output estimation when the flutter is fully developed, for the flutter induced vibration, we can observe that the steady state oscillation can be approximated by harmonic vibration with a constant amplitude.
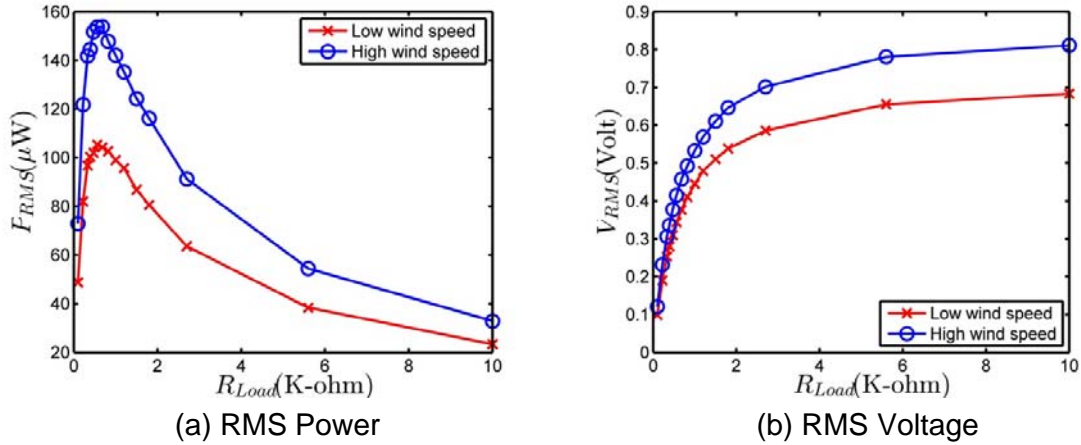

(a) RMS Power   (b) RMS Voltage

Fig. 2 Trends in power and voltage variations depending on the load resistance

Fig. 3 shows the measured voltage and the corresponding normalized power density function of voltage output from the flutter energy harvester on the field test shown in Fig. 1b. The instantaneous voltage level is almost comparable to the laboratory test; however, fluttering occurs only when wind continuously blows, wind speed is large and wind direction is almost perpendicular to the device. In addition, the normalized power spectrum density shows that structural vibrational energy due to fluttering corresponds mostly with the first bending mode.
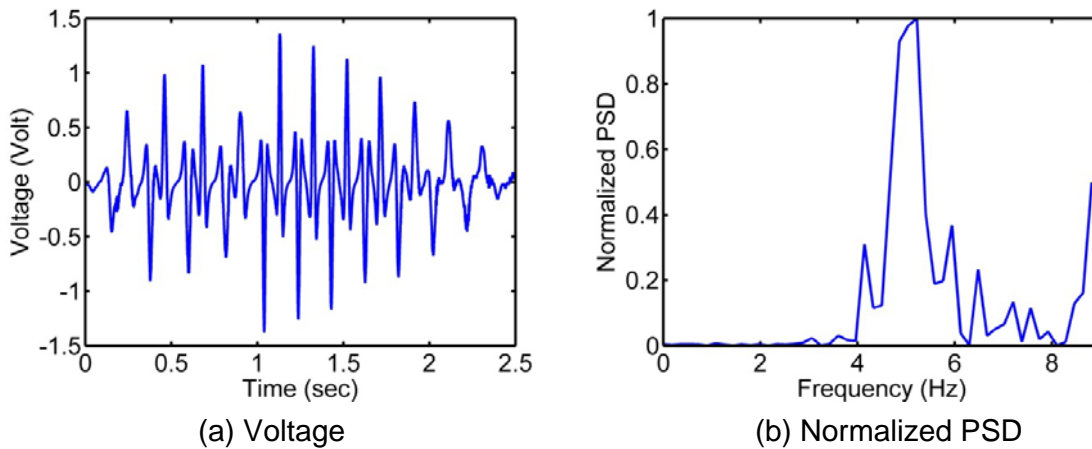

(a) Voltage   (b) Normalized PSD

Fig. 3 Field measurement

3. INTRODUCTION WIND FLOW CONTROLLING FUNNEL APPLICATION

The amount of energy produced by wind based energy harvesters is proportional to wind speed. To increase wind speed, many researchers have proposed various wind speed augmenting devices targeted on the conventional small-scale wind turbines, for example, the influence of funnel shape on the wind speed and power output gain has been studied (Capatina 2010). The efficiency of flutter based energy harvester heavily depends on the quality of wind flow. At least three conditions should be considered to initiate flutter: i) wind speed should be greater than flutter onset speed, ii) wind flow direction should be almost perpendicular to the cantilever tip, and iii) wind should blow consistently with only low level of turbulence. To make the flutter based energy harvester less sensitive to these restrictions in a real environment, we propose a wind-flow-contracting funnel device. The prototype of the funnel is shown in Fig. 4 with the installed flutter based energy harvester using the electromagnetic transducer.
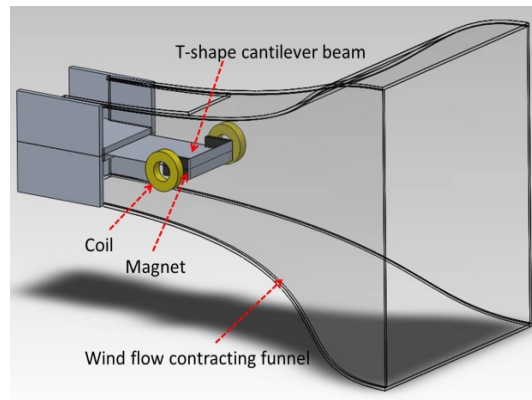

Fig. 4 Wind contracting funnel design

3.1. Influences of funnel outlet area

First, we studied the influence of the area ratio between the inlet and outlet of the funnel on wind speed and pressure variation on the outside and the inside of the funnel. We changed the funnel inlet area, while fixing the outlet area as 2×2 in^2 and funnel length as 8 in, and sampled the mean wind speed and pressure at 19 locations on the wind flow path to the device. The free stream wind speed was fixed as 4 m/s in the x direction (perpendicular to the device). The results are summarized in Fig. 5.

Outside the funnel, the wind speed decreases and the pressure increases as wind flow approaches the inlet of the funnel because of the congestion of air flow. Inside the funnel, on the contrary, the wind speed increases and the pressure decreases as wind flow approaches the funnel outlet. The general inverse relationship between wind speed and pressure follows the Bernoulli equation describing the conversion of wind flow energy:

$$P_1 + \frac{1}{2}\rho U_1^2 = P_2 + \frac{1}{2}\rho U_2^2 \qquad (12)$$

where U_1 and P_1 represent, respectively, wind speed and pressure at the initial point. U_2 and P_2 inside of the funnel, and ρ is air density. The sharp area reduction in the funnel causes air flow congested in front of the funnel, which in turn causes sharp pressure increases and wind speed reduction. The increases in speed inside of the funnel follows the continuity equation $\left(A_{in}U_{in} = A_{out}U_{out}\right)$ where A_{in} and A_{out} represent, respectively, the inlet and outlet area of the funnel.
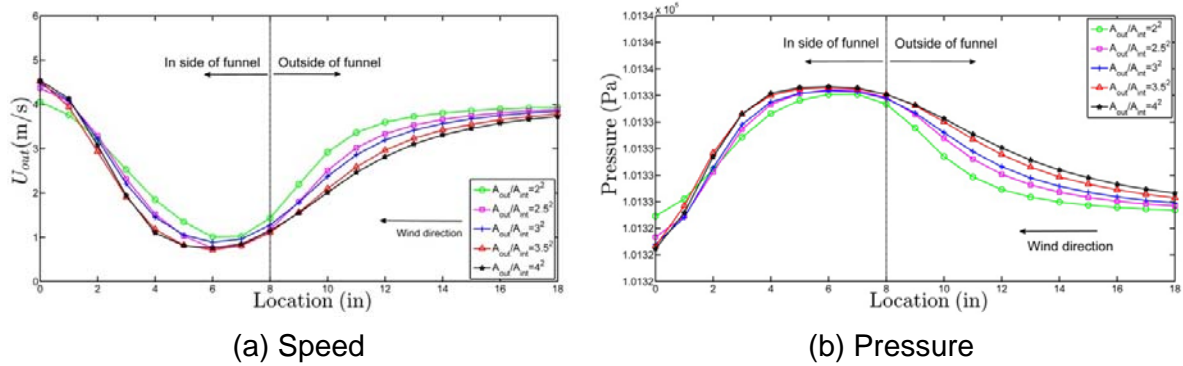

(a) Speed   (b) Pressure

Fig. 5 Mean wind speed and pressure variation with the funnel outlet area

Comparing the curves on Fig. 5a and Fig. 5b reveals that the inlet to outlet area ratio does not have considerable influences on the final wind speed gain defined as $\left(U_{out}/U_\infty\right)$ where U_∞ represents the free stream wind speed. This is because the funnel inlet area has two competing influences. Large inlet area induces large speed reduction before wind flow reaches funnel's inlet due to the increase in pressure. However, the large inlet area has large magnification effect as wind flow passes the funnel inlet according to the continuity equation.

3.2. Wind flow redirection effects of the funnel

Wind flow direction is another important factor for initiating and maintaining flutter. The wind flow contracting funnel not only magnifies wind speed but also redirects wind flow. We investigated how the funnel redirects wind flow and magnifies wind speed with different incident angles. For the simulation, we fixed the funnel design (8 in long, 4×4 in^2 inlet, and 2×2 in^2 outlet areas), and changed the incident angle of wind flow, while setting the magnitude of wind speed as 4 m/s. The CFD simulation results are summarized in Fig. 6. The colors in the figure represent the pressure distribution where darker colors correspond to higher pressure level, and the arrows represents wind speed vector.

As the wind flow incident angle increases, the level of pressure in front of the inlet attenuates, and therefore induces a slow speed reduction in front of the funnel, depicted by the change in the arrow length. The change in wind flow direction caused by the funnel is also seen as shown by the change in the arrow direction.
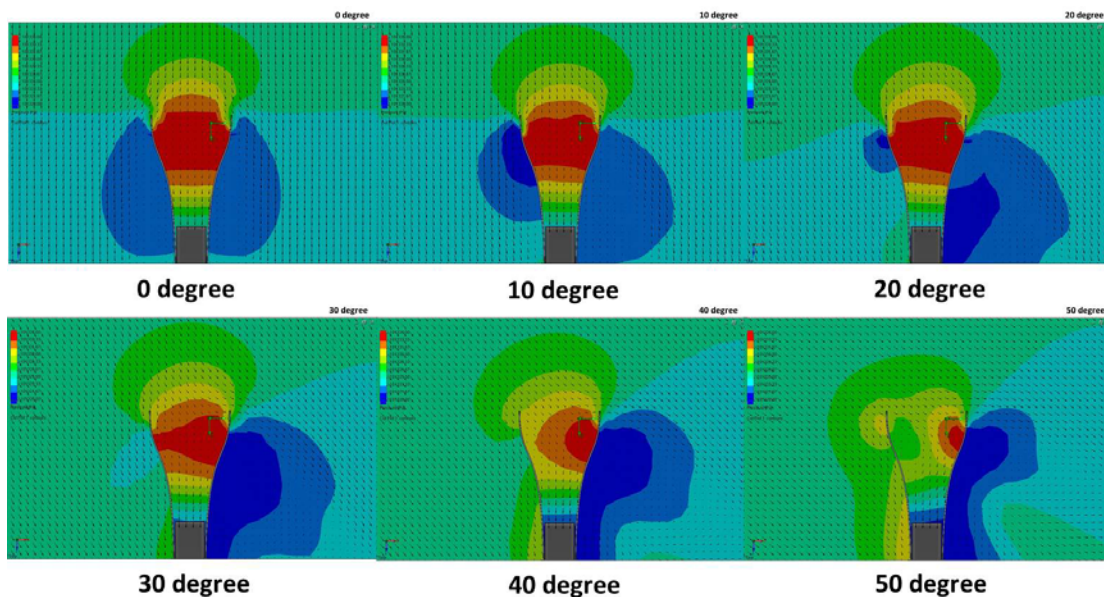
Fig. 6 Wind pressure and speed distributions with wind flow incident angles

Fig. 7 shows how the longitudinal wind speed U_X, which contributes mostly to fluttering. The pressure along with wind flow stream line changes with the incident angles. As seen in the figure, the initial longitudinal wind speed (x component of wind speed) is small when the incident angle is large; however, it is sharply magnified as wind flow passes through the funnel.

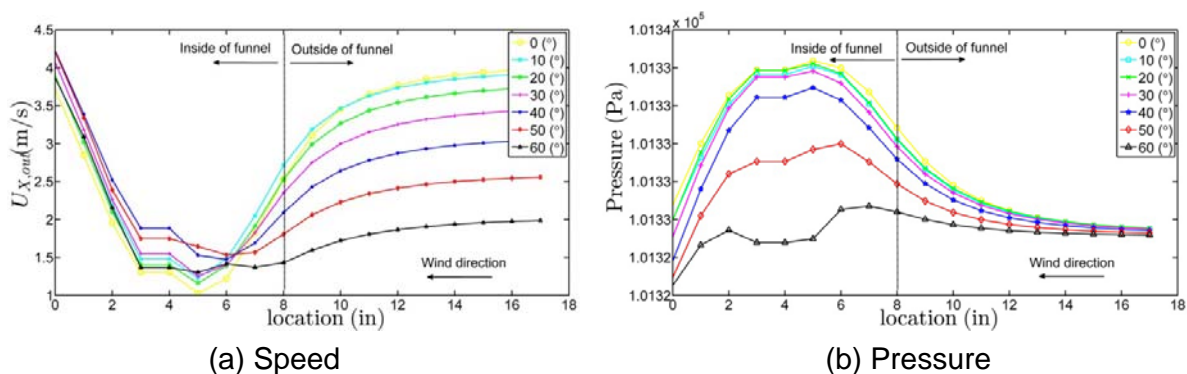(a) Speed   (b) Pressure

Fig. 7 Mean wind speed and pressure variation with wind flow incident angles

Finally, the dependency of the wind speed gains on the inlet to outlet area ratios and wind flow incident angles is summarized in Fig. 8. The overall comparison is depicted in Fig. 8a, which shows that wind speed gain logarithmically increases with the funnel inlet to outlet area ratio. The level of wind speed gain converges to approximately 10 %. The gains for total wind speed and x-directional wind speed are almost identical for each incident angle, indicating that the wind flow component deviating from the x- direction is

almost fully converted into x-directional wind flow. It is also worth noting that the wind speed gain actually increases with an increase in incident angle. This effect is advantageous to the flutter based energy harvester, as this feature can reduce the sensitivity of power output on wind flow direction which fluctuates in a real environment.
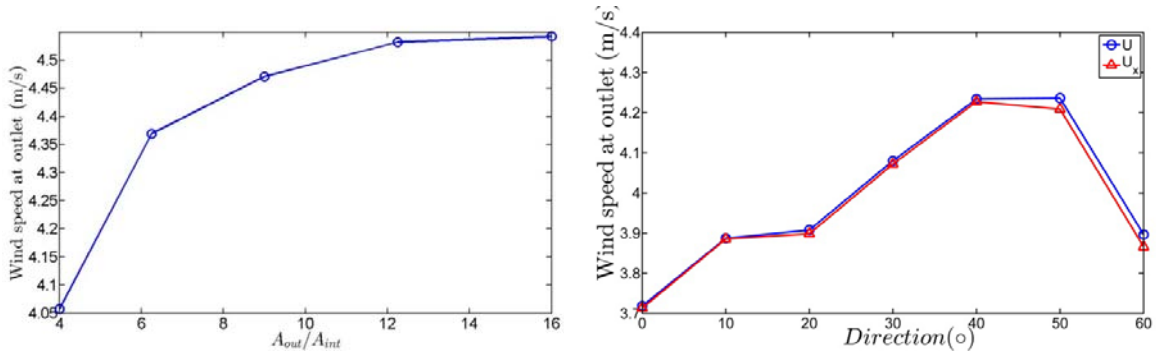
(a) Gain depending on area ratios   (b) Gain depending on incident angles

Fig. 8 Wind speed gain variations with free stream wind speeds and incident angles

3.3. Experiment results of wind contracting funnel

To validate the advantages of funnel contractility, a wind tunnel test was conducted at the KOCED wind tunnel center in Korea. Table 1 shows that how wind speed gain changes with free stream wind speed. According to the results of this test, wind speed gain is not affected by free stream wind speed U_∞ once free stream wind speed is over a certain threshold. In addition, wind tunnel tests show higher wind speed gains than the CFD simulation.

Table 1 Results of wind tunnel test on funnel's wind flow contractibility

Case	Free stream velocity		Outlet velocity		Gain
	Mean (m/s)	Turbulence intensity (%)	Mean (m/s)	Turbulence intensity (%)	$(U_{Out} - U_\infty)/U_\infty$
1	1.00	0.13	1.09	2.12	0.09
2	3.05	0.41	3.66	1.74	0.20
3	5.02	0.37	6.00	1.71	0.19
4	8.04	0.41	9.65	1.70	0.20

Next, we investigated how a wind speed gain is affected by the wind incident angles. The test results are summarized in Fig. 9a. The y-axis represents the wind speed gain estimated based on total wind speed as U_{Out}/U_∞. This result shows that funnel outlet wind speed is magnified by the funnel if the wind flow incident angle is within ± 40⁰ range. This is due to the level of pressure at the inlet of the funnel being lower when wind incident angle is not perpendicular to the funnel, which in turn reduces the wind speed decreasing rate in front of the funnel. Furthermore, wind speed component parallel to the funnel inlet surface is preserved as wind flow approaches the funnel. The widened gain band in incident angles can be advantageous to flutter based energy harvesters since it can increase the operation time of the energy harvester. Finally Fig.

9b shows the variation of the flutter onset velocities with different incident angles, demonstrating that flutter initiates at the same wind speed even though the incident angles are different.
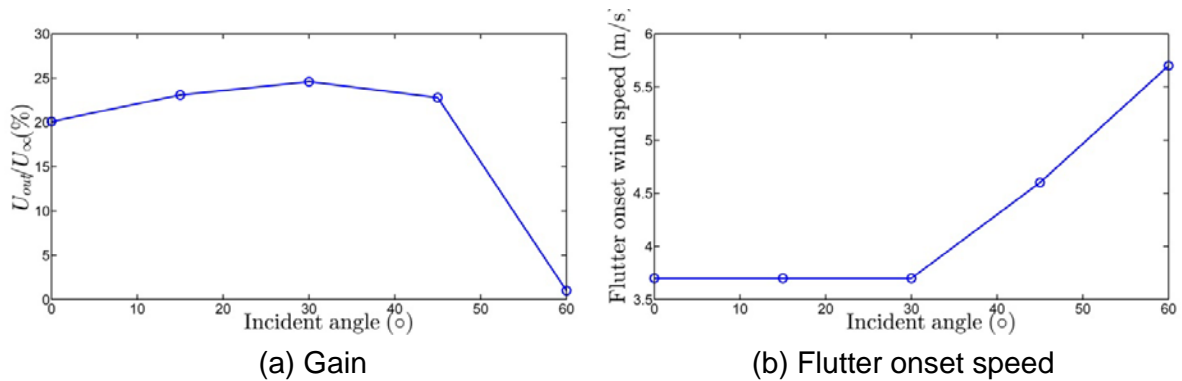

(a) Gain

(b) Flutter onset speed

Fig. 9 Gain and flutter onset speed variation with wind flow incident angles

3.4. Wind funnel influences on power outputs

We observed that the funnel effectively magnifies wind speed and redirects wind flow. To understand how this regulated wind flow affects energy harvester outputs, we conducted another wind tunnel test with the funnel mounted with a flutter energy harvester. While changing free stream wind speed from 4 m/s to 7 m/s and wind flow incident angle from 0⁰ to 40⁰, we measured the voltage output of the flutter energy harvester using NI USB 6009 DAQ driver. The wind tunnel experiment setups are shown in Fig. 10; Fig. 10a shows the flutter energy harvester without the funnel and Fig. 10b shows funnel-integrated energy harvester.
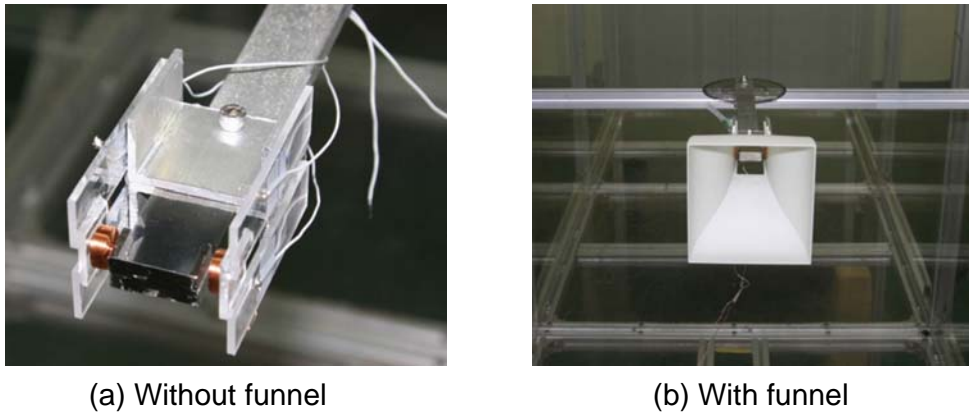

(a) Without funnel

(b) With funnel

Fig. 10 Wind tunnel test of the funnel attached to the flutter energy harvester

The test results verify that the funnel favorably affects the output of the flutter energy harvester by regulating the wind flow. Fig. 11 compares the voltage increase trends with the free stream wind speed with and without the funnel. When the incident angle is zero, in which the wind blow is perpendicular to the energy harvester, there are no distinct differences between the two cases except that the funnel slightly magnifies the

voltage. As the incident angle becomes larger (Fig. 11b and Fig. 11c), however, the trends for the two cases become clear; the funnel changes the onset speed for flutter initiation from 5 m/s to 4 m/s when the incident angle is 20⁰, and similar voltage level is maintained even when the incident angle is 40⁰, while there is no vibration observed for the case without the funnel.
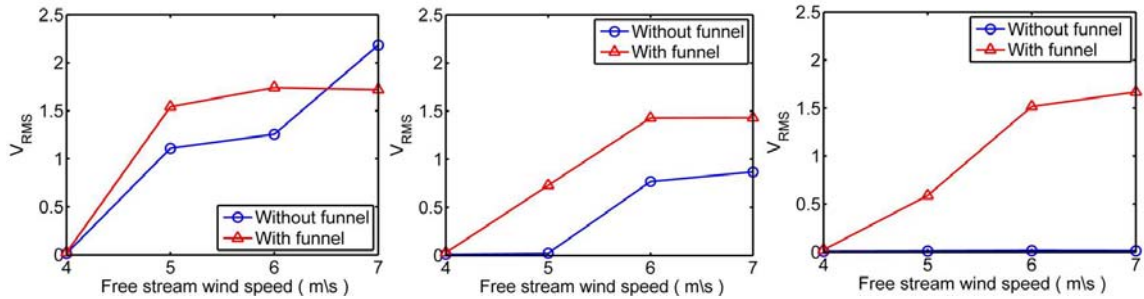
(a) Incident angle = 0⁰   (b) Incident angle = 20⁰   (c) Incident angle = 40⁰
Fig. 11 Funnel's influences on the open circuit voltage with free stream wind speeds
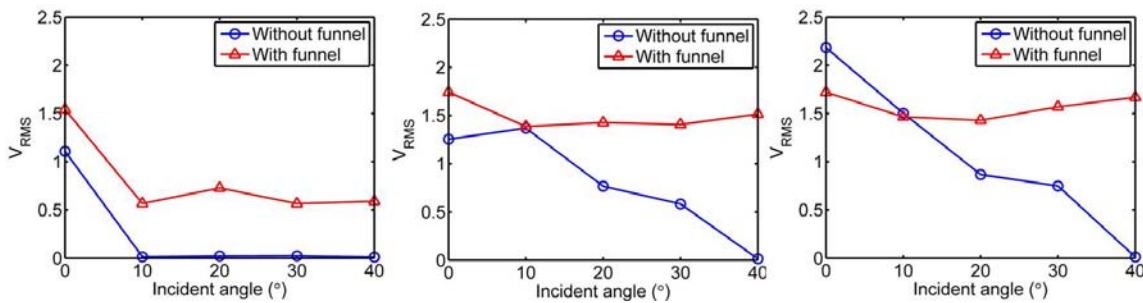
(a) $U_\infty = 5m/s$ (b) $U_\infty = 6m/s$ (c) $U_\infty = 7m/s$
Fig. 12 Funnel's influences on the open circuit voltage with Incident angles

Fig. 12 compares the variation in voltage as wind flow incident angles changes from 0⁰ to 40⁰. The results clearly show the effectiveness of the funnel in maintaining voltage outputs for different incident angles, with the three free stream wind speed cases, 5 m/s, 6 m/s, and 7 m/s. For all three free stream wind speeds, the funnel-integrated energy harvester produces almost constant level of voltage even when incident angle increases. On the other hand, the voltage output of the flutter without the funnel significantly drops as the incident angle increases.

4. CONCLUSION

The flutter based energy harvester has three advantages: it can effectively convert wind flow energy into large-amplitude mechanical vibration; there is no need for frequency matching; and the size of energy harvester can be easily reduced to a small device. However, a flutter based energy harvester has also shown the following drawbacks: it produces energy only when wind blows; and its performance is highly dependent on wind flow qualities such as speed, direction, and turbulence level. To

overcome these problems, we investigated using a wind flow contracting funnel to regulate the wind flows in front of the flutter energy harvester. The analysis and test results show that the funnel can increase wind speed by about 20 % if the incident angle is less than 30⁰, which provides higher and more consistent level of voltage output in the flutter-based energy harvester.

ACKNOWLEDGEMENT

REFERENCES

Allen, J.J. and Smith, A.J. (2001), "Energy harvesting eel." *J. Fluids Struct.,* Vol. **15**, 629–640.

Beeby, S.P. and Tudor, M.J (2006), "Energy harvesting vibration sources for microsystems application." *Meas. Sci. Technol.,* Vol. **17**(12), R175-R195.

Beeby, S.P. and Torsh, R.N (2007), "A mirco electromagnetic generator for vibration enrgy harvesting." *J. Micromech. Microeng.,* Vol. **17**(7), 1257-1265.

Bryant, M.P. and Wolff, E.N (2011), "Aeroelastic flutter energy harvester design: the sensitivity of the driving instability to system parameters." *Smart Mater. Struct.,* Vol. **20**(12) 125017

Capatina, O. and Grosan, T. (2010), "The funnel effect and its practical benefits in wind applications ", *Proceedings of '10 IEEE International Conference on Automation Quality and Testing Robotics,* Cluj-Napoca.

El-hami, M. and Glynne-Jones, P. (2001), " Design and fabrication of a new vibration-based electromechanical power generator." *Sens. Actuators, A,* Vol. **92**, 335–342.

Ge, Y.J. and Tanaka, H. (2000), "Aerodynamic flutter analysis of calble-supported bridges by multi-mode and full-mode approaches." *J. Wind Eng. Ind. Aerodyn.* Vol. **86**, 123-153.

Hung, H.J. and Kim, I.H. (2011), " An energy harvesting system using the wind-induced vibration of a stay cable for powering a wireless sensor node." *Smart Mater. Struct.* Vol. **20**, 123-153.

Kwon, S.D. (2010), "A t-shaped piezoelectric cantilever for fluid energy harvesting." *Appl. Phys. Lett.* Vol. **97**(16), 164102.

Li, S. and Yuan, J. (2011), "Ambient wind energy harvesting using cross-flow fluttering." *J. Appl. Phys.* Vol. **109**, 026104.

Roundy, S. and Wright, P.K. (2004), "A piezoelectric vibration based generator for wireless electronics." *Smart Mater. Struct.* Vol. **13**, 1131-1142.

Scanlan, R.H. (1978), " The action of flexible bridges under wind, i: Flutter theory." *J. Sound Vib.* Vol. **60**(2), 187–199.

Stærdahl, J. and Winther, J. (2007), "Aeroelastic stability of suspension bridges using CFD", *Proceedings of '07 International Symposium of the International Association for Shell and Spatial Structures,* Venice.

Sun, C. and Shi, J. (2011), " PVDF microbelts for harvesting energy from respiration." *Energy and Environmental Science.* Vol. **4**, 4508-4512.

Wright, J.R. and Cooper, J.E. (2007), *Introduction to Aircraft Aeroelasticity and Loads*, John Wiley and Sons, Ltd.